THE JOURNAL OF PHYSICAL CHEMISTRY B

 VOLUME 108, NUMBER 46, NOVEMBER 18, 2004

LETTERS

High-Yield Catalytic Synthesis of Thin Multiwalled Carbon Nanotubes

Hee Jin Jeong,[†] Ki Kang Kim,[†] Seung Yol Jeong,[†] Min Ho Park,[‡] Cheol Woong Yang,[‡] and Young Hee Lee*,[†]

Department of Physics, Institute of Basic Science, National Research Laboratory for Carbon nanotubes, Center for Nanotubes and Nanostructured Composites, Sungkyunkwan University, Suwon 440-746, Republic of Korea, and Department of Advanced Materials Engineering, Center for Nanotubes and Nanostructured Composites, Sungkyunkwan University, Suwon 440−746, Republic of Korea

Received: August 26, 2004; In Final Form: October 12, 2004

We have synthesized thin multiwalled carbon nanotubes (t-MWNTs) using a catalytic chemical vapor deposition (CCVD) method with FeMoMgO catalyst. The number of tube walls were 2∼6 with the corresponding diameters of 3∼6 nm. We obtained high production yield of over 3000 wt % compared to the weight of the supplied catalyst. These t-MWNTs revealed the intermediate structural characteristics between single- and multiwalled carbon nanotubes (SWNTs and MWNTs). Critical issues for high yield synthesis of t-MWNTs were further discussed in terms of reduction procedure, growth time, and gas species.

Introduction

In addition to an early synthesis of SWNTs and MWNTs,[1,2] double-walled carbon nanotubes (DWNTs) have been synthesized recently.[3−6] Despite strong applicability of nanotubes, applications are still limited by their electronic and atomic structures. For example, large field enhancement factor, high conductivity, and high durability of emission tip are necessary for an efficient field emitter. SWNTs have been reported to provide a large field enhancement factor, low threshold voltage, and high emission currents,[7] but the substantial degradation of emission currents has been shown to be a serious bottleneck for the application of SWNT-based field emission display (FED).[8] In contrast with SWNTs, MWNTs have shown high emission stability but small field enhancement factor. DWNTs could be an alternative for this purpose but the poor production rate and the redundant purification process have been a serious drawback.[9] In this report, we have synthesized t-MWNTs that are composed of 2∼6 walls. The maximum production rate of nanotubes is as high as 3000 wt % compared to the weight of the supplied catalysts, and the minimum weight of FeMoMgO-containing catalysts after nanotube synthesis is lower than 3.5 wt % without purification process. These t-MWNTs could be a good candidate as ultimate field emitters and for other applications.

Experimental Section

FeMoMgO catalysts were prepared by combustion synthesis.[10] Aqueous solution of iron nitrate (99.99%, Aldrich), magnesium nitrate (99.99%, Aldrich), and ammonium molybdate (99.98%, Aldrich) in a molar ratio of $Fe_{0.1}Mo_{0.025}Mg_{0.875}O$, which is the best composition for high-yield nanotube synthesis in our experiments, were mixed together. Citric acid (4 g) was added to the prepared solution as a foaming and combustion additive, then mild sonication and stirring followed. The mixture was directly loaded into the furnace and fired at 550 °C for 5 min. After the combustion process, the produced foaming materials were ground using a mortar. These FeMoMgO powders with the specific surface areas of 20 m^2/g were loaded

* Corresponding author. E-mail: leeyoung@skku.edu.
[†] Department of Physics, Institute of Basic Science, National Research Laboratory for Carbon nanotubes.
[‡] Department of Advanced Materials Engineering.

10.1021/jp046152o CCC: $27.50
Published on Web 10/26/2004

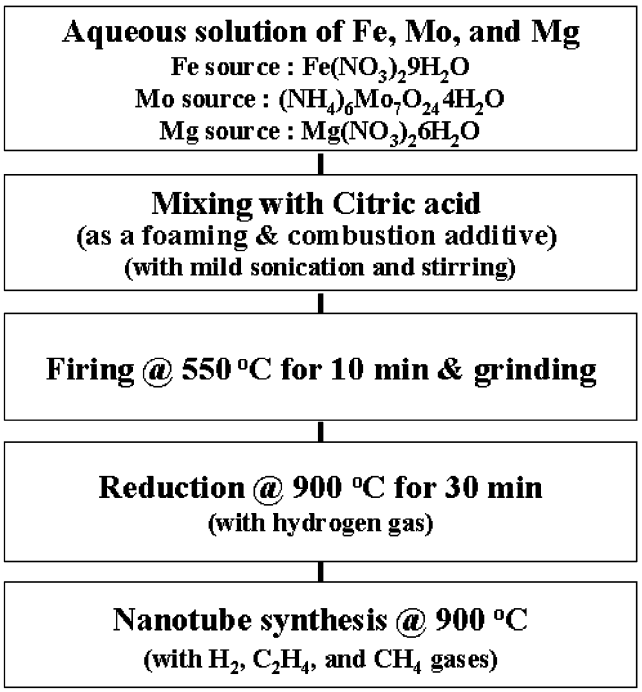

Figure 1. Schematic diagram of the experimental procedure for catalyst preparation and nanotube synthesis.

immediately into the CVD chamber. The in situ reduction process of the catalyst powder by flowing hydrogen gas (900 °C for 30 min) decreased the catalyst mass by 37 wt %. Thin MWNTs were then synthesized at the same temperature with a gas mixture of hydrogen, methane, and ethylene under an atmospheric pressure. The schematic diagram of our experimental procedure was shown in Figure 1. The flow rate of hydrogen gas was fixed at 500 sccm in all experiments. Argon gas at a rate of 1000 sccm was flowed during the heating-up to 900 °C and the cooling-down to room temperature. In this experiment, growth parameters such as growth time and gas ratio of ethylene/methane were varied for high yield synthesis of t-MWNTs.

We used thermogravimetric analysis (TGA) to evaluate the purity and yield of t-MWNTs. Before the TG measurement, the sample was preheated to 200 °C in N_2 atmosphere. The TG measurement [Seiko Exstar 6000(TG/DTA6100)] was done in air with a heating rate of 2 °C/min from room temperature up to 1000 °C. We used Fourier transform (FT) Raman (Bruker IFS-66/S) with Nd:YAG laser (excitation wavelength of 1064 nm) and Rayleigh line rejection filter with a spectral range of 70−3600 cm^{-1} for Stokes shift. The sample morphology was observed by field-emission scanning electron microscopy (FESEM) (JSM6700F, JEOL). The diameter and structure of t-MWNTs were measured by high-resolution transmission electron microscopy (HRTEM) (JEM-3011, JEOL).

Results and Discussion

Figure 2a shows the photo image of the FeMoMgO powder spread over the ceramic boat with an inner size of 4 cm × 1 cm × 1 cm before reduction. The boat was overflowed with nanotubes when methane gas was flowed for 30 min at 900 °C, as shown in Figure 2b. The soot product was multiplied by about 1350 wt % compared to the originally reduced catalyst. Figures 2c and 2d show the typical FESEM images of the as-grown t-MWNTs. The MgO particles are hardly visible from all of the FESEM images taken from many different spots, which is quite reasonable due to the high volumetric ratio of

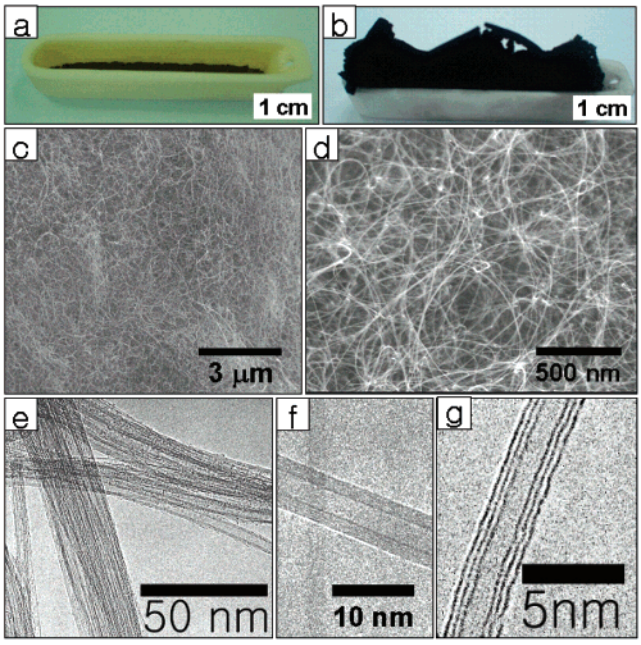

Figure 2. Photo images of the ceramic boat with FeMoMgO catalyst (a) before and (b) after the nanotube synthesis. (c), (d) FESEM images and (e)−(g) HRTEM images of as-grown carbon nanotubes.

nanotubes to catalysts, despite the presence of catalyst amount of 3.5 wt %. The nanotube density is very high. Nanotubes are usually long without the observable tube ends similar to SWNTs. The bundle size seems to be rather narrow compared to those of SWNTs and DWNTs.[1,11] Figures 2e−2g show a series of images from HRTEM. Nanotubes are usually straight with rather small bundle sizes, as shown in Figure 2e, in good agreement with the SEM images. Nanotubes are mostly clean without amorphous carbon particles on the tube walls, consistent with the results of TGA and Raman spectra that will be discussed later. The diameters of the outer walls range from 3 to 6 nm. Some nanotubes have rather large inner diameters of 3 nm, as shown in Figure 2f. Although these nanotubes have a small number of walls, SWNTs are hardly observable in several HRTEM images.

Figure 3a demonstrates the distribution of the number of nanotube walls. The most probable number of walls is four. It is well known that the nanotube diameters are determined by the size of the catalyst.[12] Our results suggest that the catalysts are very uniformly distributed over the MgO supporter, which is the main role for the metal oxide supporter, and consistent with the previous reports.[3,9,13] Figure 3b shows the TG and differential TG of the as-grown sample in air atmosphere. The sample starts burning near 500 °C and ends burning near 650 °C. The remaining quantity is 6.8 ± 0.3 wt %, which is the mass of oxidized catalyst with MgO supporter. This value is quite low, compared to the previous CCVD using other types of catalysts.[14] This amount could further be reduced by improving the yield. Our as-grown sample could be used directly as field emitters and most composites without further purification. The differential TG shows a narrowly distributed peak with a slightly asymmetric component at the lower temperature side. The inset shows that this peak is composed of four Gaussian curves with peaks centered at 538, 570, 597, and 622 °C. The burning temperature of nanotubes is related to the number of walls, quality of nanotubes, presence of catalysts, and even bundle size in the case of SWNTs.[15,16] The reported burning temperature of the CVD-grown SWNTs within zeolite pores was around 580 °C,[14] as high as that of the purified DWNTs

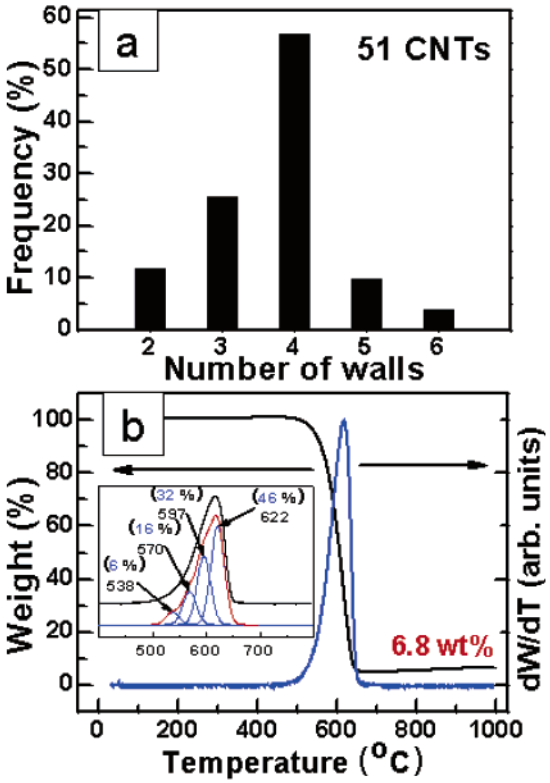

Figure 3. (a) Distribution of the number of nanotube walls measured from TEM observations and (b) TG and DTG of as-grown carbon nanotubes.

grown by arc discharge.[17] SWNTs grown by the zeolite template have usually small bundle sizes that will decrease the burning temperature. Therefore, high burning temperature indicates high crystal quality. The burning temperature of the arc dischage grown SWNTs was 480 °C, whereas this temperature was increased to 550 °C after purification.[17] This increment of the burning temperature was attributed to the formation of bundles and removal of catalysts. By neglecting the effect of small amount of catalysts and small bundle sizes in our t-MWNTs, we attribute the variance of the burning temperatures to the presence of different numbers of the nanotube walls in the sample.

Figures 4a and 4b show the yield of nanotubes (mass of the total product/mass of the catalyst including MgO supporter after reduction) as a function of growth time and ethylene/methane flow rate ratio, respectively. In Figure 4a, the flow rate of methane gases was fixed to 500 sccm. 90 wt % of nanotubes were produced during an early stage of 30 min with respect to the 120 min. The high yield of 1450 wt % nanotubes was obtained at 2 h of growth time using the methane gases without ethylene gases. Ethylene gas is generally known to be less stable than methane gas.[18] This means that ethylene gas can be easily decomposed at high growth temperature, and the decomposed carbon atoms increase enough with increasing the flow rate of ethylene gas, enhancing the nanotube yield. For this reason, we increased the flow rate of ethylene gas with respect to the methane, as shown in Figure 4b. In this case, we fixed the growth time at 120 min. As the ethylene/methane ratio increases, the nanotube yield increases continuously. We emphasize here that the yield reaches 3050 wt % at an ethylene/methane ratio of 10%. This is extremely high, compared to the previous reports of less than 280 wt %.[9] This high yield of t-MWNTs is contributed from two factors: (i) a large number of available catalyst sites and (ii) efficient catalytic reactivity. In the

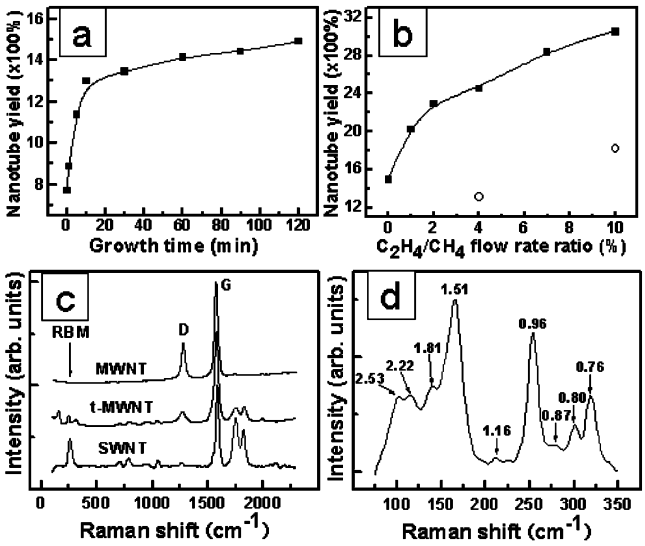

Figure 4. Nanotube yield in terms of (a) the growth time and (b) the ratio of flow rate of ethylene and methane gases. (c) Raman spectra of CVD-grown single-, thin-, and multiwalled CNTs and (d) the corresponding RBM of the t-MWNTs.

FeMoMgO catalyst, the role of each species is different. The Fe catalysts are well distributed on the corrugated MgO supporter and are prevented from being aggregated, which results in maintaining their small sizes during high-temperature synthesis (see the Supporting Information). The Fe catalysts with high density play a crucial role in obtaining the high yield of nanotubes. The Mo particles act as a promoter to increase the nanotube yield. To increase the catalytic reactivity, the reduction process of catalyst is an essential step. In our case, we achieved this by performing both reduction and the subsequent nanotube synthesis in the same chamber. This prohibits reoxidation of catalysts such that highly efficient catalytic reactivity is maintained and at the same time all the reduced catalyst could be utilized for nanotube synthesis. To prove this, catalyst reduction was done separately and brought into the growth chamber such that the reoxidation takes place during the transfer of the catalyst. We found that the yield dropped significantly, as shown by the open circles in Figure 4b. On the other hand, because the saturation behavior did not occur at an ethylene/methane ratio of 10%, the nanotube yield might be increased at a larger ethylene/methane ratio. However, the co-products such as amorphous carbon particles and thick MWNTs could be also obtained. Therefore, the high yield synthesis of the pure t-MWNTs should be optimized with care.

Figure 4c shows the FT-Raman spectra of various samples with an excitation wavelength of 1064 nm. The integration intensity of the D-band of our t-MWNTs near 1320 cm^{-1} is slightly larger than that of the CVD-grown SWNTs but much smaller than that of MWNTs. This suggests that our t-MWNTs have high crystallinity similar to SWNTs. Figure 4d shows the radial breathing mode (RBM) of the as-grown t-MWNTs. The presence of RBM indicates that our t-MWNTs have inner diameter ranges of 0.7−2.6 nm similar to SWNTs. We used the expression $\nu(cm^{-1}) = 9 + 235/d$ (nm) to calculate the diameter from the RBM signal.[19] Some large diameters among these RBMs do not necessarily originate from the inner walls. Because of the limit of the Notch filter used in FT-Raman, we cannot observe RBMs below 100 cm^{-1}. Therefore, the diameter distribution from TEM observations and Raman spectra will be quite different from each other for large-diameter nanotubes, particularly with diameters greater than 3 nm. As a result of

the Raman analysis, our t-MWNTs reveal the intermediate structural characteristics between SWNTs and MWNTs.

Conclusion

We have demonstrated very high yield synthesis method for thin MWNTs using CCVD with an FeMoMgO catalyst. A large number of available catalyst sites and efficient catalytic reactivity are two crucial factors to control. The catalytic reactivity was maximized by performing the reduction of catalyst and consecutive synthesis of nanotubes in the same chamber. The yield was also controlled in terms of growth time and the mixing ratio of methane/ethylene gases.

Acknowledgment. This work was supported in part by the Ministry of Science and Technology (MOST) through National Research Laboratory (NRL) and in part by the Center for Nanotubes and Nanostructured Composites at SKKU.

Supporting Information Available: Figure S1. HRTEM images of FeMoMgO catalyst produced by combustion synthesis. This material is available free of charge via the Internet at http://pubs.acs.org.

References and Notes

(1) Bethune, D. S.; Kiang, C. H.; de Vries, M. S.; Gorman, G.; Savoy, R.; Vasquez, J. *Nature* **1993**, *363*, 605.
(2) Iijima, S. *Nature* **1991**, *354*, 56.
(3) Flahaut, E.; Peigney, A.; Laurent, Ch.; Rousset, A. *J. Mater. Chem.* **2000**, *10*, 249.
(4) Smith, B. W.; Luzzi, D. E. *Chem. Phys. Lett.* **2000**, *321*, 169.
(5) Bandow, S.; Takizawa, M.; Hirahara, K.; Yudasaka, M.; Iijima, S. *Chem. Phys. Lett.* **2001**, *337*, 48.
(6) Hutchison, J. L.; Kiselev, N. A.; Krinichnaya, E. P.; Krestinin, A. V.; Loutfy, R. O.; Morawsky, A. P.; Muradyan, V. E.; Obraztsova, E. D.; Sloan, J.; Terekhov, S. V.; Zakharov, D. N. *Carbon* **2001**, *39*, 761.
(7) Choi, W. B.; Chung, D. S.; Kang, J. H.; Kim, H. Y.; Jin, Y. W.; Han, I. T.; Lee, Y. H.; Jung, J. E.; Lee, N. S.; Park, G. S.; Kim, J. M. *Appl. Phys. Lett.* **1999**, *75*, 3129.
(8) Uemura, S.; Yotani, J.; Nagasako, T.; Kurachi, H.; Yamada, H.; Ezaki, T.; Maesoba, T.; Nakao, T. *SID 02 DIGEST* **2002**, 1132.
(9) Saito, Y.; Nakahira, T.; Uemura, S. *J. Phys. Chem. B* **2003**, *107*, 931.
(10) Patil, K. C. *Bull. Mater. Sci.* **1993**, *16*, 533.
(11) Wei, J.; Ci, L.; Jiang, B.; Li, Y.; Zhang, X.; Zhu, H.; Xu, C.; Wu, D. *J. Mater. Chem.* **2003**, *13*, 1340.
(12) Ren, Z. F.; Huang, Z. P.; Xu, J. W.; Wang, J. H.; Bush, P.; Siegal, M. P.; Provencio, P. N. *Science* **1998**, *282*, 1105.
(13) Jeong, H. J.; An, K. H.; Lim, S. C.; Park, M. S.; Chang, J. S.; Park, S. E.; Eum, S. J.; Yang, C. W.; Park, C. Y.; Lee, Y. H. *Chem. Phys. Lett.* **2003**, *380*, 263.
(14) Murakami, Y.; Miyauchi, Y.; Chiashi, S.; Maruyama, S. *Chem. Phys. Lett.* **2003**, *374*, 53.
(15) Moon, J. M.; An, K. H.; Lee, Y. H.; Park, Y. S.; Bae, D. J.; Park, G. S. *J. Phys. Chem. B* **2001**, *105*, 5677.
(16) An, K. H.; Jeon, K. K.; Moon, J. M.; Eum, S. J.; Yang, C. W.; Park, G. S.; Park, C. Y.; Lee, Y. H. *Synth. Met.* **2004**, *140*, 1.
(17) Lee, J. Y.; Kim, D. Y.; Jeong, H. J.; Lim, S. C.; Hwang, H. S.; Han, J. H.; Lee, Y. H., submitted to *Phys. Rev. B* **2004**.
(18) Kong, J.; Cassell, A. M.; Dai, H. *Chem. Phys. Lett.* **1998**, *292*, 576.
(19) Pfeiffer, R.; Kuzmany, H.; Kramberger, Ch.; Schaman, Ch.; Pichler, T.; Kataura, H.; Achiba, Y.; Kürti, J.; Zólyomi, V. *Phys. Rev. Lett.* **2003**, *90*, 225501.